

# Drying in Porous Media: Equilibrium and Non-equilibrium Approaches for Composting Processes

Pujol<sup>\*1,3</sup>, Pommier<sup>2</sup>, Debenest<sup>3</sup>, Quintard<sup>3</sup> and Chenu<sup>1</sup>

<sup>1</sup> Veolia Environnement, <sup>2</sup> INSA Toulouse, <sup>3</sup> IMFT

\*Corresponding author: Allée du Professeur Camille Soula 31400 TOULOUSE (FRANCE), pujol@imft.fr

**Abstract:** A composting model including reactive transfers, a biological model and taking into account the drying phenomena has been developed at the Darcy scale (see Figure 1). The model has been implemented under COMSOL Multiphysics®. Different simulations have been carried out to compare results obtained with local non-equilibrium or local equilibrium assumptions describing the gas/liquid water exchange. The two approaches appear to be equivalent under certain conditions and local non-equilibrium has been chosen preferably because it allows for shorter calculation times and easy implementation. Tests carried out with this formulation point out the importance of drying in the control of organic matter biodegradation, therefore drying phenomena must be taken into account in composting models.

**Keywords:** drying, modeling, local non-equilibrium, composting, porous media.

## 1. Introduction

Composting is a process whereby biodegradable organic material from wastes is converted into a stable granular material called compost. The biodegradation of this organic fraction is operated by aerobic micro-organisms, which consume oxygen from air and organic matter to produce carbon dioxide, water and heat. This leads to a rise in temperature over several consecutive days allowing the sanitation of the product. Applying the obtained compost to land improve soil structure and enrich the soil nutrient content.

From an industrial point of view, composting consists in controlling the organic waste biodegradation in order to reduce stabilization times. Since the efficiency of industrial composting processes is largely controlled by oxygen availability within the waste, the acceleration of the biological activity is generally obtained by improving oxygen input into waste

piles by turning compost windrow and/or by injecting air into the compost (forced injection).

Nevertheless, the overall efficiency of the process is also controlled by environmental factors, described in Figure 1. Among them, one of the most important seems to be the moisture content (Diaz *et al.*, 2007). For example, lack of water within the waste slows down the degradation. Conversely, a medium where the matter moisture content is too important impedes the oxygenation, thus the decomposition.

Since moisture content is one of the most influent parameter on the biological activity, it seems essential to understand and control it in order to ensure an efficient composting. Hence, this paper presents the development of a model that takes into account heat and mass transport phenomena coupled with aerobic biodegradation and drying. The model is implemented under COMSOL Multiphysics® and different local equilibrium and non-local equilibrium approaches are evaluated to simulate drying phenomena at the Darcy's scale. The model is then used to simulate impact of drying on the composting process, when no external water is added to the waste.

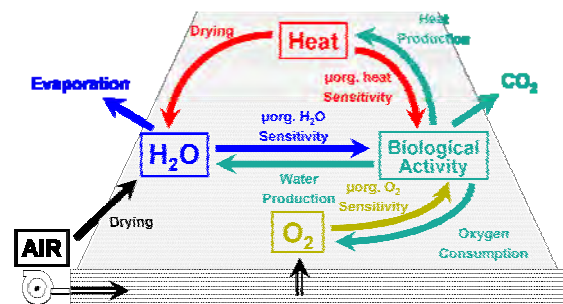


Figure 1. Schematic representation of the different couplings involved in composting processes.

## 2. Drying Phenomenon

In a compost windrow where a forced aeration is used occurs a classical convective drying as defined by Mujumdar *et al.* (2000).

This drying has an important role in the composting process whose effectiveness depends on the amount of liquid water necessary for micro-organisms to ensure the degradation of organic matter. Therefore, prediction of drying impact on compost moisture content evolution is a crucial need.

At equilibrium, there is a relationship between the material moisture content and the gas phase vapour concentration. In the absence of specific data, the equation of the sorption isotherm used in this paper is the one suggested by Oswin (1946) and is given by:

$$\text{BET} = \frac{\left( \frac{\omega_{\text{H}_2\text{O},l}}{A(1-\omega_{\text{H}_2\text{O},l})} \right)^{\frac{1}{B}}}{1 + \left( \frac{\omega_{\text{H}_2\text{O},l}}{A(1-\omega_{\text{H}_2\text{O},l})} \right)^{\frac{1}{B}}} \quad (1)$$

Figure 2 represents this sorption isotherm for wood.

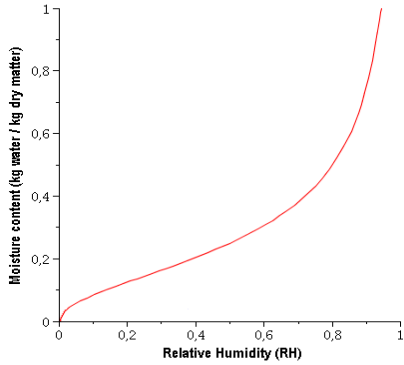


Figure 2. Example of curve of a sorption isotherm from the expression of Oswin for wood (1946)

### 3. Model development

The developed model takes into account reactive transport in porous media, biological mechanisms and the drying phenomenon. The problem is a multiscale problem as illustrated in Figure 3. The developed model is a Darcy-scale one. The upscaling procedure to obtain this model is not presented in this paper and we refer the reader to the literature on the subject (Puiggali et al., 1992; Quintard and Whitaker, 1988; Whitaker 1998; Golfier et al., 2009). The

Darcy-scale governing transport equations are listed below.

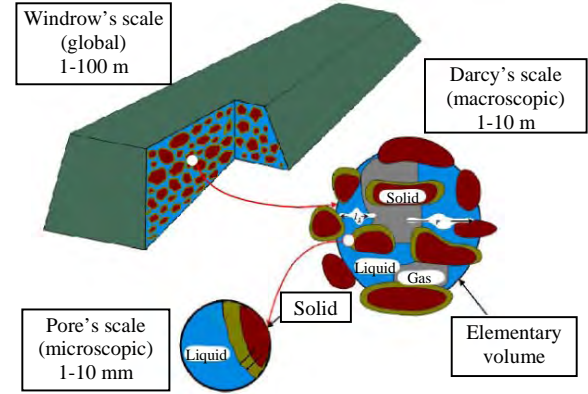


Figure 3. Different scales to be considered when applying up-scaling procedure to composting model.

#### 3.1 Model presentation

The equation of mass conservation in the gas phase is described by:

$$\frac{\partial(\epsilon_g \rho_g)}{\partial t} + \vec{\nabla} \cdot (\epsilon_g \rho_g \vec{u}_g) = \dot{m} + R_{\text{O}_2,g} + R_{\text{CO}_2,g} \quad (2)$$

where  $\vec{u}_g$  is the Darcy's velocity given by:

$$\vec{u}_g = -\frac{\kappa_a}{\epsilon_g \eta_g} (\vec{\nabla} P - \rho_g \vec{e}_z) \quad (3)$$

In Equation (2),  $\dot{m}$  is a mass exchange term between the gas phase and the liquid phase for water.  $R_{\text{O}_2,g}$  and  $R_{\text{CO}_2,g}$  are terms from the biological activity for the oxygen consumption and carbon dioxide production.

It has been chosen to use the ideal gas assumption:

$$\rho_g = \frac{PM}{RT} \quad (4)$$

where the mixture molar mass is given by :

$$M = \frac{1}{\sum_{i=1}^n \frac{\omega_{i,g}}{M_i}} \quad (5)$$

Equation (2) describes the global conservation of the gas phase. In order to monitor the

composition evolution of this phase, it is necessary to consider the mass conservation of gas species: oxygen, nitrogen and carbon dioxide.

$$\frac{\partial(\varepsilon_g \rho_g \omega_{i,g})}{\partial t} + \bar{\nabla} \cdot (\rho_g \bar{u}_g \omega_{i,g}) = \bar{\nabla} \cdot (\varepsilon_g \rho_g D_g^* \bar{\nabla} \omega_{i,g}) + R_{i,g} \quad (6)$$

The equation for water vapor is given by:

$$\frac{\partial(\varepsilon_g \rho_g \omega_{H_2O,g})}{\partial t} + \bar{\nabla} \cdot (\rho_g \bar{u}_g \omega_{H_2O,g}) = \bar{\nabla} \cdot (\varepsilon_g \rho_g D_g^* \bar{\nabla} \omega_{H_2O,g}) + \dot{m} \quad (7)$$

Water can be found in the gas phase but it is mainly present in the liquid phase where the mass conservation of water is described by Equation (8):

$$\frac{\partial(\varepsilon_l \rho_l \omega_{H_2O,l})}{\partial t} = -\dot{m} + R_{H_2O,l} \quad (8)$$

where we made the assumption that the liquid water is immobile given the low saturation. This approximation is based on the few amounts of leachate produced in composting plants.  $R_{H_2O,l}$  is the term of water creation due to the degradation of organic matter.

The mass fraction of gas water in equilibrium with the liquid phase is given by:

$$\omega_{H_2O,g,eq} = \frac{P_{sat}}{P} M_{H_2O} \sum_{i=1}^n \frac{\omega_{i,g}}{M_i} BET \quad (9)$$

BET is the term representing the sorption isotherm governing the equilibrium between the liquid phase and the gas phase for water (see Equation (1))

The local equilibrium heat conservation equation is given by:

$$\left( \varepsilon_g \rho_g C_{pg} + \varepsilon_l \rho_l C_{pl} + \varepsilon_s \rho_s C_{ps} \right) \frac{\partial T}{\partial t} + \varepsilon_g C_{pg} T \frac{\partial \rho_g}{\partial t} + \rho_g C_{pg} (\bar{u}_g \bar{\nabla}) T = \bar{\nabla} \cdot (\lambda^* \bar{\nabla} T) - \dot{m} \Delta H_{vap} + R_T \quad (10)$$

where  $\Delta H_{vap}$  is the enthalpy of vaporization of water.  $R_T$  is the heat production due to the biological activity.

Finally, the biological model is inspired from the one developed by Pommier *et al.* (2008). It takes into account three solid fractions: the first one is rapidly biodegradable ( $X_{Rb}$  ( $\text{kg.m}^{-3}$ )), the second one is slowly biodegradable ( $X_{Sb}$  ( $\text{kg.m}^{-3}$ )), and the third one is inert ( $X_I$  ( $\text{kg.m}^{-3}$ )). The two first fractions are progressively transformed in a rapidly hydrolysable fraction ( $S_r$  ( $\text{kg.m}^{-3}$ )) directly assimilated by bacteria ( $X_a$  ( $\text{kg.m}^{-3}$ )). Mortality of these bacteria creates inert material and rapidly biodegradable solid fraction. All these phenomena are described by Equation (11) to Equation (15):

$$\frac{\partial X_{Rb}}{\partial t} = -\gamma_T \tau k_{Rh} X_{Rb} + \gamma_T \tau \varphi_{O_2} (1-f_1) b X_a \frac{0.844}{0.706} \quad (11)$$

$$\frac{\partial X_{Sb}}{\partial t} = -\gamma_T \tau k_{Sh} X_{Sb} \quad (12)$$

$$\frac{\partial X_I}{\partial t} = \gamma_T \tau \varphi_{O_2} f_1 b X_a \frac{0.844}{0.706} \quad (13)$$

$$\frac{\partial X_a}{\partial t} = \gamma_T \tau \varphi_{O_2} \mu_{max} \frac{S_r}{K_{S_r} + S_r} X_a - \gamma_T \tau \varphi_{O_2} b X_a \quad (14)$$

$$\frac{\partial S_r}{\partial t} = \gamma_T \tau k_{Rh} X_{Rb} \frac{0.9375}{0.844} + \gamma_T \tau k_{Sh} X_{Sb} \frac{0.9375}{0.844} - \gamma_T \tau \varphi_{O_2} \frac{\mu_{max}}{Y_a} \frac{S_r}{K_{S_r} + S_r} X_a \frac{0.9375}{0.844} \quad (15)$$

$\gamma_T, \tau$  and  $\varphi_{O_2}$  are limitation terms of the biodegradation due to thermal effect (Rosso *et al.*, 1993), moisture limitation effect (Pommier *et al.*, 2008) and oxygen availability (Mason, 2007).

In this paper, two different implementations of the conceptual model are considered whether the local equilibrium assumption (LE) or the local non-equilibrium assumption (LNE) are used for describing the water exchange between the gas and liquid phases.

### 3.2 LE or LNE: definitions

For the local equilibrium assumption, the diffusion at the pore-scale is instantaneous, in comparison with the characteristic time of convection. Therefore, the average gas water

concentration is equal to the interface equilibrium concentration given by the sorption isotherms.

If local non-equilibrium is considered, the water exchange term between the gas phase and the liquid phase is given by:

$$\dot{m} = \varepsilon_g \rho_g \sigma (\omega_{\text{H}_2\text{O,g,eq}} - \omega_{\text{H}_2\text{O,g}}) \quad (16)$$

The equilibrium kinetic is there controlled by the parameter  $\sigma$ .  $\sigma$  is inversely proportional to the relaxation time required to obtain the equilibrium within the pore space. Its value depends on the pore geometry, the value of the diffusion coefficient value in the gas phase, and other numerous factors. The local non-equilibrium model leads to a spreading of the drying front compared to the local equilibrium situation. The adjustment of  $\sigma$  allows controlling the front thickness: a high value implies a sharp front while a low value will spread the front. Therefore, it is possible to control the value of  $\sigma$  in order to obtain results close to those obtained with LE assumption.

## 4. Results

### 4.1 Model set-up

The geometry used for the simulations is a two-dimensional slice of a 100L cylindrical composting reactor filled with waste.

Wastes can be considered as a mixture of wood and sludge. The values of all the parameters are the same for the two models.

The initial moisture content is around 62% (Luo *et al.*, 2008; Ahn *et al.*, 2007) while the moisture content at the boundary is defined thanks to the average annual relative humidity in France which is around 78%. Then, the sorption isotherm gives the moisture content to be applied at inlet boundary.

Referring to Gao *et al.* (2010), the initial temperature of the waste has been chosen around 22°C. The air injection temperature is chosen to be around 12°C, which is the annual mean temperature in France. A convective heat flux described by Equation (19) is imposed to the external pilot envelop.

$$f = h(T - T_\infty). \quad (19)$$

The initial oxygen concentration has been chosen according to data from Ahn *et al.* (2007). The oxygen inlet concentration is set to be equal to normal oxygen concentration in the air.

The biological parameters are those used by Sole-Mauri *et al.* (2007) and Pommier *et al.* (2008).

Finally, the air inlet velocity is taken to be  $1.10^{-3}$  m.s<sup>-1</sup> (M. Gao *et al.*, 2009; Ahn *et al.*, 2007).

### 4.2 Observation of differences between LE and LNE

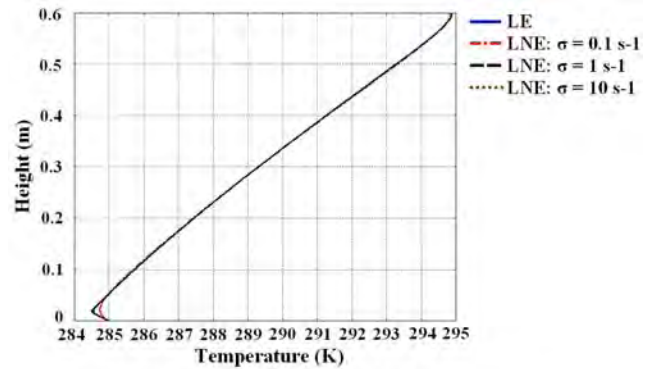


**Figure 4.** Comparison of temperature profiles along the domain between LE and the LNE models (t=14 days)

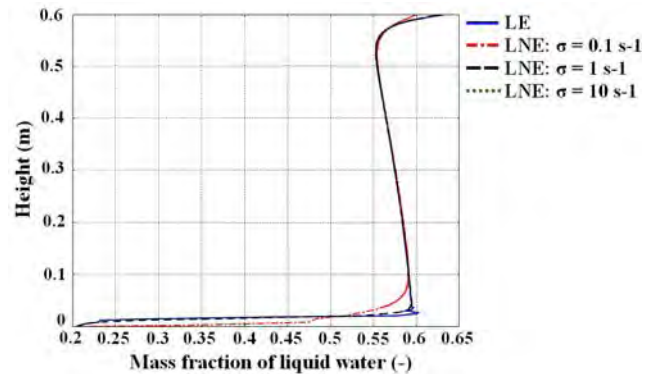


**Figure 5.** Comparison of mass fraction of liquid water profiles along the domain between the LE model and the LNE models (t=14 days)

For the local non-equilibrium model, the parameter  $\sigma$  controls the equilibrium kinetic. Three different values of  $\sigma$  were used, in order to appreciate its impact on the simulations, and

compare the results with those obtained with the local equilibrium assumption. The tests are run for  $\sigma = 0.1\text{s}^{-1}$ ,  $\sigma = 1\text{s}^{-1}$  and  $\sigma = 10\text{s}^{-1}$ .

The simulations are carried out on a period of 14 days (which is generally the testing time on pilots). All the figures presented illustrate the variables in the axis of symmetry of the geometry.

The results obtained for the temperature and the mass fraction of liquid water are given in Figure 4 and Figure 5.

First, it can be noticed that, after 14 days of simulation, the temperature profiles (Figure 4) of the LNE models match very well the temperature profile of the LE model, except for  $\sigma = 0.1\text{s}^{-1}$  near the domain entrance.

Then, concerning the liquid water mass fraction profiles (Figure 5, the LNE model with  $\sigma = 0.1\text{s}^{-1}$  and the LE model are quite different along the first 10 cm and at the top of the domain. With  $\sigma = 1\text{s}^{-1}$ , LE and LNE results almost the same shape, while with  $\sigma = 10\text{s}^{-1}$ , LE and LNE match perfectly.

Finally, the calculations for the LE model have lasted 35 min while the calculations for the LNE model last 28 min ( $\sigma = 0.1\text{s}^{-1}$ ), 26 min ( $\sigma = 1\text{s}^{-1}$ ) and 30 min ( $\sigma = 10\text{s}^{-1}$ ), on the same computer. Calculations times become even more important for bigger geometries (proportional to the domain size).

So the local non-equilibrium model seems more interesting than the local equilibrium one in term of computational load. This may be explained by the fact that the LNE model offers a diffuse interface modelling for LE situations which are marked by very sharp fronts. The LNE solution is smoother and continuous, thus allowing for a better convergence of the numerical implementation.

### 4.3 Equivalence between LE and LNE for a range of $\sigma$

In this part, values of  $\sigma$  for which the local non-equilibrium model is a good approximation of the local equilibrium situation are investigated.

For  $\sigma \in [1; 4]$ , the local non-equilibrium model and the local equilibrium model can be considered equivalent, and these values of  $\sigma$  do not create numerical problems. Moreover, the calculations are faster for the LNE model than with the local equilibrium model.

Therefore, the future simulations will be done with a local non-equilibrium model and an intermediate value for  $\sigma$ ,  $\sigma = 2.5\text{s}^{-1}$ .

### 4.4 Impact of drying on the composting process

Air with lower moisture content is injected in the massif of waste in order to understand the impact of drying. No external water is added to the waste. The results are then compared to those obtained with a test where the previously parameters was set.

A relative humidity of 40% is chosen for the injected air. Figure 6 and Figure 7 illustrate the obtained results.

The amount of consumed organic matter is less important when a dry air is injected (Figure 6). After 14 days of simulation, 0.15 kg more have been consumed in the reference case (which represents 15% more). Additionally, the drying front has moved quickly (more rapid drying) and the domain is dryer for the dry injected air case (Figure 7). Finally, the amount of gas evaporated which goes out of the domain is equal to 5.8 kg for the reference case, and 6.3 kg (8% more with a dry air).

## 5. Conclusions

In this paper, the development of a Darcy-scale composting model has been presented. This model is used to better understand the impact of drying on the process. It takes into account transfer of water in the gas and liquid phases, oxygen, carbon dioxide and nitrogen in the gas phase, and heat transfer. A biological model has also been included to couple the consumption and production of some chemical species to the

production of heat due to biological activity.

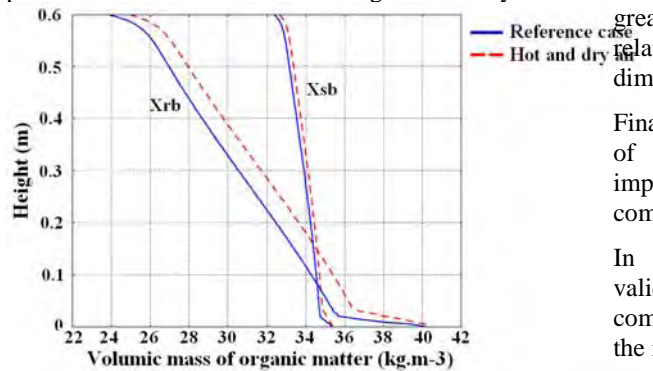


**Figure 6.** Comparison of biodegradable organic matter profiles along the domain between the reference case (previous set of parameters) and an injection of a dry air ( $t=14$  days)

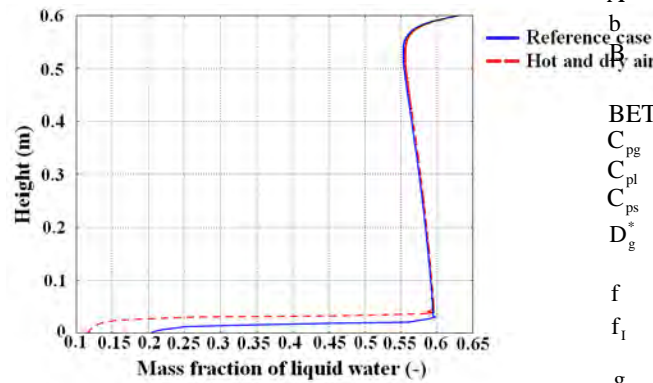


**Figure 7.** Comparison of mass fraction of liquid water profiles along the domain between the reference case (previous set of parameters) and an injection of a dry air ( $t=14$  days)

Moreover, the model takes into account drying phenomena through a water exchange term between the liquid and the gas phases.

Then, local equilibrium and local non-equilibrium assumption for water phase change have been assessed. Simulations have pointed out that the LNE model is faster than the LE one and allows an easier numerical implementation. Additionally, the two models give equivalent results for sufficiently large values of the exchange coefficient.

Finally, tests have been carried out to highlight the impact of drying on the composting process. Around 8% of water vapour has been additionally evaporated when injecting a hot and dry air. The amount of consumed organic matter is more important with a moist air with 15%

additional degraded. This amount could become greater depending on the temperature and relative humidity of the injected air and on the dimension of the pile.

Finally, model results points out that the effects of drying on the composting process are important and need to be taken into account in composting models.

In order to confirm these conclusions, validation tests will be carried out later, comparing experimental or literature data with the model's results.

## 6. Nomenclature

A	coefficient of the sorption isotherm	-
b	death constant	$s^{-1}$
B	coefficient of the sorption isotherm	$m^2 \cdot m^{-3}$
BET	sorption isotherm	-
$C_{pg}$	specific heat capacity of gas	$J \cdot K^{-1}$
$C_{pl}$	specific heat capacity of liquid	$J \cdot K^{-1}$
$C_{ps}$	specific heat capacity of solid	$J \cdot K^{-1}$
$D_g^*$	diffusion coefficient in the gas phase	$m \cdot s^{-1}$
f	convective heat flux	$W \cdot m^{-2}$
$f_1$	percentage of dead bacteria becoming inert matter	$s^{-1}$
g	gravity acceleration	$m \cdot s^{-2}$
h	exchange coefficient	$W \cdot K^{-1} \cdot m^{-1}$
$k_{Rh}$	rapidly hydrolysis constant	$s^{-1}$
$k_{Sh}$	slowly hydrolysis constant	$s^{-1}$
$K_{Sr}$	coefficient of aerobic population apparent affinity for organic substrate	$kg \cdot m^{-3}$
M	molar mass	$kg \cdot mol^{-1}$
$M_i$	molar mass of the gas specie I	$kg \cdot mol^{-1}$
$\dot{m}$	exchange term between the gas phase and the liquid phase	$kg \cdot m^{-3} \cdot s^{-1}$
P	pressure	Pa
$P_{sat}$	vapor pressure	Pa
R	ideal gas constant	$J \cdot mol^{-1} \cdot K^{-1}$
$R_{H_2O,l}$	production term of water	$kg \cdot m^{-3} \cdot s^{-1}$
$R_{i,g}$	source term from biological activity	$kg \cdot m^{-3} \cdot s^{-1}$
$R_T$	production term of heat	$kg \cdot m^{-3} \cdot s^{-1}$
$S_r$	rapidly hydrolysable substrate	$kg \cdot m^{-3}$
T	temperature	K
$T_\infty$	outside temperature	K
t	time	s
$\bar{u}_g$	Darcy's velocity	$m \cdot s^{-1}$
$X_a$	bacterial population	$kg \cdot m^{-3}$
$X_1$		

	inert inorganic particles	$\text{kg.m}^{-3}$
$X_{\text{Rb}}$	rapidly biodegradable substrate	$\text{kg.m}^{-3}$
$X_{\text{Sb}}$	slowly biodegradable substrate	$\text{kg.m}^{-3}$
$Y_a$	conversion efficiency of substrate into biomass	-

#### Greek letters

$\varepsilon_g$	porosity	-
$\varepsilon_l$	$1 - \varepsilon_g$	-
$\gamma_T$	limitation term of biodegradation under temperature effect	-
$\kappa_a$	permeability	$\text{m}^2$
$\lambda^*$	equivalent thermal conductivity	$\text{W.m}^{-1}.\text{K}^{-1}$
$\mu_{\text{max}}$	specific rate of growth	$\text{s}^{-1}$
$\eta_g$	dynamic viscosity in gas	$\text{kg.m}^{-1}.\text{s}^{-1}$
$\phi_{\text{O}_2}$	limitation term of biodegradation under the influence of oxygen availability	-
$\rho_g$	gas density	$\text{kg.m}^{-3}$
$\rho_l$	liquid density	$\text{kg.m}^{-3}$
$\sigma$	adjustment parameter	$\text{s}^{-1}$
$\tau$	limitation term of biodegradation under moisture effect	-
$\omega_{\text{H}_2\text{O},g}$	mass fraction of liquid water	-
$\omega_{i,g}$	mass fraction of gas specie i	-
$\Delta H_{\text{vap}}$	vaporization enthalpy	$\text{J.kg}^{-1}$

#### Subscripts

g	gas
i	gas species ( $\text{O}_2$ , $\text{CO}_2$ , $\text{N}_2$ , $\text{H}_2\text{O}$ )
l	liquid
s	solid

## 7. References

- Ahn, H. K., T. L. Richard and H. L. Choi, Mass and thermal balance during composting of a poultry manure – Wood shavings mixture at different aeration rates, *Process Biochemistry*, Vol. 42, pp. 215-223, (2007).
- Diaz, L. F. and G. M. Savage, Factors that affect the process, Elsevier, 49, (2007).
- Gao, M., B. Li, A. Yu, F. Liang, L. Yang and Y. Sun, The effect of aeration rate on forced-aeration composting of chicken manure and sawdust, *Bioresource Technology*, Vol. 101, pp. 1899-1903, (2010).
- Golfier, F., B. D. Wood, L. Orgogozo, M. Quintard and M. Buès, Biofilms in porous media: Development of macroscopic transport equations via volume averaging

with closure for local mass equilibrium conditions, *Adv. Wat. Res.*, Vol. 32, pp. 463-485, (2009).

- Luo, W., T. B. Chen, G. D. Zheng, D. Gao, Y. A. Zhang and W. Gao, Effect of moisture adjustments on vertical temperature distribution during forced-aeration static-pile composting of sewage sludge, *Resources, Conservation and Recycling*, Vol. 52, pp. 635-642, (2008).
- Mason, I. G., An evaluation of substrate degradation patterns in the composting process. Part 2: Temperature-corrected profiles, *Waste Management*, (2007).
- Mujumdar, A. S. and S. Devahastin, *Fundamental principles of drying*, Exergex, Brossard, Canada, (2000).
- Oswin, G. R., The kinetics of package life, *Industrial Chemistry*, Vol. 65(28), pp. 419-442, (1946).
- Pommier, S., D. Chenu, M. Quintard and X. Lefebvre, Modelling of moisture-dependant aerobic degradation of solid waste, *Waste Management*, Vol. 28(7), pp. 1188-1200, (2008).
- Puiggali, J. R. and M. Quintard, Properties and simplifying assumptions for classical drying models, in *Advances in Drying* (ed. By A. S. Mujumdar, chapter 4, pp. 109-143), Hemisphere Publishing Corporation, Washington (USA), (1992).
- Quintard, M. and S. Whitaker, Two-phase flow in heterogeneous porous media: The method of large-scale averaging, *Transport in Porous Media*, Vol. 3(4), pp. 357-413, (1988).
- Rosso, L., J. R. Lobry and J. P. Flandrois, An unexpected correlation between cardinal temperatures of microbial growth highlighted by a new model, *Journal of Theoretical Biology*, Vol. 162, pp 447-463, (1993).
- Sole-Mauri, F., J. Illa, A. Magrí, F. X. Prenafeta-Boldú and X. Flotats, An integrated biochemical and physical model for the composting process, *Bioresource Technology*, Vol. 98, pp. 3278-3293, (2007).
- Withaker, S., *The Method of Volume Averaging*, Kluwer Academic Publishers, The Netherlands, (1998).